Geochimica et Cosmochimica Acta, Vol. 69, No. 18, pp. 4425–4436, 2005
Copyright © 2005 Elsevier Ltd
Printed in the USA. All rights reserved
0016-7037/05 $30.00 + .00

doi:10.1016/j.gca.2005.04.003

Clay mineral weathering and contaminant dynamics in a caustic aqueous system I. Wet chemistry and aging effects

Sunkyung Choi, Mary Kay Amistadi and Jon Chorover*

Department of Soil, Water and Environmental Science, University of Arizona, Tucson, AZ, 85721 USA

(*Received July* 23, 2004; *accepted in revised form April* 8, 2005)

Abstract—Caustic high level radioactive waste induces mineral weathering reactions that can influence the fate of radionuclides released in the vicinity of leaking storage tanks. The uptake and release of Cs^{I} and Sr^{II} were studied in batch reactors of 2:1 layer-type silicates—illite (Il), vermiculite (Vm) and montmorillonite (Mt)—under geochemical conditions characteristic of leaking tank waste at the Hanford Site in WA (0.05 *m* Al_T, 2 *m* Na^+, 1 *m* NO_3^-, pH ~14, Cs and Sr present as co-contaminants). Time series (0 to 369 d) experiments were conducted at 298 K, with initial $[Cs]_0$ and $[Sr]_0$ concentrations from 10^{-5} to 10^{-3} mol kg^{-1}. Clay mineral type affected the rates of (i) hydroxide promoted dissolution of Si, Al and Fe, (ii) precipitation of secondary solids and (iii) uptake of Cs and Sr. Initial Si release to solution followed the order Mt > Vm > Il. An abrupt decrease in soluble Si and/or Al after 33 d for Mt and Vm systems, and after 190 d for Il suspensions was concurrent with accumulation of secondary aluminosilicate precipitates. Strontium uptake exceeded that of Cs in both rate and extent, although sorbed Cs was generally more recalcitrant to subsequent desorption and dissolution. After 369 d reaction time, reacted Il, Vm and Mt solids retained up to 17, 47 and 14 mmol kg^{-1} (0.18, 0.24 and 0.02 μmol m^{-2}) of Cs, and 0, 27 and 22 mmol kg^{-1} (0, 0.14 and 0.03 μmol m^{-2}) Sr, respectively, which were not removed in subsequent Mg exchange or oxalic acid dissolution reactions. Solubility of Al and Si decreased with initial Cs and Sr concentration in Mt and Il, but not in Vm. High co-contaminant sorption to the Vm clay, therefore, appears to diminish the influence of those ions on mineral transformation rates. *Copyright © 2005 Elsevier Ltd*

1. INTRODUCTION

Accidental leakage of high level radioactive waste (HLRW) into the subsurface has occurred at several Department of Energy (DOE) sites, including the Hanford Site, WA, the Savannah River Site, GA, and the Oak Ridge Site, TN, because of waste tank overfilling, transfer line breakage and tank failure (McKinley et al., 2001). This has resulted in the introduction of highly-caustic, radionuclide-containing solutions into underlying sediments and soils. At the Hanford Site, the bulk of the radioactivity released to the vadose zone is present as ^{137}Cs and ^{90}Sr in concentrations up to parts per million (Serne et al., 2001a). Radionuclides ^{137}Cs and ^{90}Sr are nuclear fission products that present a particular concern due to their high fission yields (6.18 and 5.77%) and long half-lives of 30.2 and 28.8 yr, respectively. As a result of high reactive surface site density and high specific surface area, clay-sized mineral particles may retard the migration of these radionuclides in receiving sediments via adsorption and/or surface precipitation reactions (McKinley et al., 2002; Steefel et al., 2003).

As a borderline Lewis acid of low ionic potential (z/r = 6 nm^{-1}), Cs^+ does not form strong complexes with hard Lewis base ligands, including surface hydroxyl groups of metal oxide surfaces. Instead, sorption to basal and interlayer surfaces of layer silicate clays tends to control its environmental fate (Kim et al., 1996). To a greater degree than smaller cations in group 1A (Li, Na), Cs forms inner-sphere complexes on charged ditrigonal siloxane sites that are similar in diameter to that of the ionic adsorbate (Maes and Cremers, 1978; Kim and Kirkpatrick, 1997; Bostick et al., 2001; Sutton and Sposito, 2001). Such surface complexes are favored by the low Cs^+ hydration enthalpy (−263 kJ mol^{-1}). Like K^+, Cs^+ exhibits a high affinity for frayed-edge sites (FES) on partially weathered mica and illite, resulting in selectivity coefficients (K_{ex}) for Ca^{2+} Cs^+ exchange as high as 7×10^{-10} (Comans et al., 1991; Zachara et al., 2002). External basal and interlayer surfaces of expansible 2:1 layer-type clays (smectite and vermiculite) are also important sorption sites in soils (Oscarson et al., 1987). Charge location in the tetrahedral sheet (e.g., vermiculite) promotes greater inner-sphere complexation relative to octahedral sheet charge (e.g., montmorillonite) (Bailey, 1980; Douglas, 1989; Bostick et al., 2001; Sutton and Sposito, 2001). This range in site selectivity is such that adsorption kinetics at circumneutral pH and low ionic strength are characterized by a fast initial step followed by slower uptake over longer time period (months) consistent with diffusion to high affinity sites (Torstenfelt et al., 1982; Comans et al., 1991; Poinssot et al., 1999). At neutral pH and in the presence of the high Na^+ (> 1.0 M) concentrations encountered in HLRW, Cs^+ adsorption to Hanford (Ringold) sediments from 10^{-9} to 10^{-2} M Cs solutions was limited to high-affinity FES sites (Zachara et al., 2002). Increasing temperature above 298 K diminishes site selectivity for Cs^+ over Na^+ while enhancing Cs desorption kinetics (Liu et al., 2003a, 2003b).

The smaller Sr^{2+} cation is a hard Lewis acid that exhibits a higher hydration enthalpy (−1445 kJ mol^{-1}) and ionic potential (17 nm^{-1}) approaching those of Ca^{2+} (−1592 kJ mol^{-1} and 20 nm^{-1}, respectively). As with Ca^{2+}, adsorption to a wide range of mineral surfaces—including layer silicates and hydrous oxides—occurs dominantly via outer-sphere complexation, consistent with an ion exchange mechanism (Chen et al.,

* Author to whom correspondence should be addressed (chorover@cals.arizona.edu).

1998; Oscarson and Hume, 1998; Sahai et al., 2000; O'Day et al., 2000). Strontium adsorption to layer silicate clays at circumneutral pH is thought to be reversible and outer-sphere (Rafferty et al., 1981; Puls et al., 1989; Gutierrez and Fuentes, 1993; Dyer et al., 2000; Lu and Mason, 2001). Jeong et al. (1996) reported higher uptake of Cs than Sr by illite and smectite, and ascribed the difference to the higher hydration energy of Sr.

Although most prior studies have focused on Cs and Sr adsorption reactions at circumneutral pH and low ionic strength, the high pH (13–14), ionic strength (> 2 M) and Al concentrations (*ca.* 0.01–0.2 M) of HLRW solutions (Serne et al., 1998; 2001a) are known to favor rapid dissolution of silicates and neoformation of zeolitic and feldspathoid solids on time scales that are relevant to contaminant uptake (Bickmore et al., 2001; Chorover et al., 2003, 2004; Choi et al., in press). The fate of radionuclides in this dynamic geochemical environment is poorly understood, but could involve adsorption-desorption on native mineral surfaces, as well as co-precipitation with, or adsorption to, solid-phase products of incongruent dissolution. Cesium and Sr are sequestered into distinct solid phase products of kaolinite dissolution under these conditions (Chorover et al., 2003). However, the coupled sorption and weathering behavior that occur in caustic-waste systems comprising 2:1 layer-type silicates, with much higher cation exchange capacity, have not been reported previously. Smectite is the dominant 2:1 layer-type silicate at shallow depths in Hanford soils. Illite and vermiculite are also present in this zone, proximal to the tanks (from muscovite and biotite weathering), and they increase in prevalence with increasing depth (Serne et al., 2001b).

To better understand geochemical processes governing contaminant fate, there is a clear need for experimental data on long-term weathering and contaminant sorption behavior of clay minerals in the caustic aqueous environment characteristic of the vadose zone bordering the source zone. The objective of the present research was to establish linkages between mineral solubility and sorptive uptake of Cs and Sr to 2:1 layer-type silicates (illite, vermiculite and smectite) and their secondary weathering products during reaction with a synthetic tank waste leachate for reaction times up to one year. Geochemical conditions for this study are representative of the "near-field" environment underneath the leaking tank. Mineral transformations are discussed in detail in a companion paper (Choi et al., 2005).

2. MATERIALS AND METHODS

2.1. Preparation of Stock Clay Suspensions

Montmorillonite (SWy-2) from Crook County, WY and illite (IMt-1) from Silver Hill, MT (both dioctahedral) were obtained from the Source Clays Repository of the Clay Minerals Society. Trioctahedral vermiculite from Phalaborwa in Transvall of South Africa was obtained from Ward's Scientific Inc., NY. All clays were size fractionated and cleaned before experiments. The <2 μm montmorillonite (Mt) fraction was collected by repeated sedimentation-resuspension and cleaned to remove oxide impurities by sequential repeated washings in ultrapure (MilliQ) water adjusted pH 9.5 with 0.01 M NaOH, then with 1.0 M NaCl adjusted to pH 3 with 0.1 M HCl, and finally with 0.01 M NaCl until the equilibrium pH was 5.5 (Chorover et al., 2003). Illite (IL) and vermiculite (Vm) were prepared according to the method of Sposito and LeVesque (1974) with slight modifications. Two hundred grams of illite were transferred to an agate mortar and particle size was reduced by gentle tapping with an agate pestle. For vermiculite, large flakes were ground in a ball mill for less than 5 min. Powdered samples were transferred to 1 L polypropylene bottles containing 750 mL of Milli-Q water and placed on a reciprocating shaker at low speed for 2 h. The clay suspensions were then transferred to a 2 L beaker, allowed to stand undisturbed for 5 min and the particles remaining in suspension were collected by aspiration. The sedimented material was resuspended in MilliQ water on a reciprocating shaker for 20 min, and this procedure was repeated until the suspensions were clear. A 1 M NaCl solution was added to give a final concentration of 0.01 M NaCl. Particles of Stokes diameter <115 μm were isolated by sedimentation and the volume of collected suspension was reduced by centrifugation. The supernatant solution measured pH 8.8 without base addition. The isolated fraction was suspended in 1.0 M NaCl at pH 3 on a reciprocal shaker for 2 h. This step was repeated until the supernatant solution was pH 3. To avoid excess mineral dissolution, the suspension did not remain at pH <5.0 for longer than the 2 h shaking time (Sposito and LeVesque, 1974). The clays were then redispersed and washed repeatedly in 0.01 M NaCl adjusted to pH 7 until the pH value of the supernatant solution reached pH 6 to 7. All Na-saturated clay suspensions were stored at (4°C).

Subsamples of the purified clay were taken for total elemental analysis by ICP-OES and ICP-MS following Li-metaborate fusion (Sawhney and Stilwell, 1994). These data were used to calculate the layer silicate structural formulae (Cîcêl and Komadel, 1994). Trace quantities of quartz in all clay suspensions and anatase in illite, as detected by XRD, were accounted for in determination of the structural formulae. Conventional mineralogical characterization (K and Mg saturation, ethylene glycol and glycerol solvation, and heat treatments) of the vermiculite sample by XRD indicated that the purified sample contained no detectable illite interstratification or hydroxy-interlayering. Total specific surface areas of the purified clays were determined using the ethylene glycol monoethyl ether (SSA_{EGME}) adsorption method (Pennell, 2002). Cesium accessible structural charge was measured as in Chorover et al. (1999).

2.2. Kinetic Batch Experiments

The use of glassware was avoided at all stages to prevent Si contamination. Reagent grade $NaNO_3$, NaOH, CsCl, $SrCl_2 \cdot 6H_2O$, and $NaAlO_2 \cdot \times H_2O$ were used as obtained from VWR Scientific Inc. (West Chester, PA). A consistent, CO_2 free background solution (solution concentrations prepared and reported on a mass basis) composed of ultrapure (MilliQ) water with 2.0 mol kg^{-1} Na^+, 1 mol kg^{-1} NO_3^-, 1 mol kg^{-1} OH^- and 0.05 mol kg^{-1} Al_T was prepared to simulate the chemistry of Hanford tank waste leachate (Serne et al., 1998). The synthetic tank waste leachate (STWL) was spiked to give three initial aqueous phase Cs^+ and Sr^{2+} concentrations, where each contaminant was added at a solution concentration of 10^{-5}, 10^{-4} or 10^{-3} mol kg^{-1}, and both cations were present at equal concentration in all systems to compare co-contaminant fate. Batch experiments were conducted in sealed 60 mL polypropylene copolymer (PPCO) bottles. All suspension clay concentrations were 20.0 g kg^{-1} (0.50 g dry mass in 25.0 g of STWL) to give similar total moles of Si in each batch reactor, and the following initial suspension interfacial areas (based on SSA_{EGME}) in m^2 $g^{-1}{}_{solution}$: 1.86 (illite), 3.92 (vermiculite), and 14.0 (montmorillonite). Six replicate reactors were used for each treatment and time-step to provide duplicate sets for (i) wet chemistry analysis, (ii) solid phase analysis after reaction, and (iii) solid phase analysis after postreaction acid ammonium oxalate extraction. Blank controls included two types: those with no clay added and those with no clay or Al added, to assess the potential for carbonate formation and Al hydroxide precipitation on Cs and Sr uptake. No carbonate or Al hydroxide solids were formed in the controls. All solutions were initially undersaturated with respect to Al precipitates (e.g., boehmite, gibbsite) and carbonate solids (strontianite).

The batch reactors were placed on an end-over-end shaker at 2 rpm and replicate sets were sampled after 1, 7, 33, 93, 190 and 369 d. At the termination of a given reaction period, suspensions were allowed to settle for 97 min and then 10 g of suspension were sampled from the top 2.2 cm by pipette to yield a composite sample containing suspended colloidal material (< 2 μm effective Stokes diameter) and dissolved

Table 1. Chemical formulae and specific surface areas of the Na-saturated clays.

Clay Mineral	Chemical Formula[1]	Specific Surface Area[2] [$m^2\ g^{-1}$]
Illite (IMt-1)	$K_{1.27}Na_{0.14}\ [Si_{7.34}Al_{0.66}]\ (Al_{2.72}Fe^{3+}_{0.34}Fe^{2+}_{0.35}Mg_{0.42}Ti_{0.11})\ O_{20}\ (OH)_4$	93.1 ± 0.71
Vermiculite	$Ca_{0.02}K_{0.02}Na_{1.20}[Si_{6.05}Al_{1.65}Fe^{3+}_{0.30}]\ (Al_{0.01}Fe^{3+}_{0.40}Fe^{2+}_{0.16}Mg_{5.24}Mn_{0.01}Ti_{0.11})\ O_{20}\ (OH)_4$	196 ± 7.9
Montmorillonite (SWy-2)	$K_{0.02}Na_{0.66}\ [Si_{7.95}Al_{0.05}]\ (Al_{3.0}Fe^{3+}_{0.36}Fe^{2+}_{0.03}Mg_{0.44}Ti_{0.01})\ O_{20}\ (OH)_4$	702 ± 38

[1] Calculated from total elemental analysis of Na-saturated clays.
[2] Specific surface area measured by ethylene glycol monoethyl ether (EGME) adsorption

solutes. This sample was then acidified before analysis of "colloidal plus dissolved" metals. Suspensions were then transferred quantitatively to PPCO tubes and centrifuged at 28,700 *g* for 20 min. The supernatant solution was filtered through a 0.2 μm PTFE syringe filter and acidified to pH 1.5 with trace metal grade HNO_3 before analysis of "dissolved" metals. The centrifuged pellets were resuspended in 95% ethanol (adjusted to pH 10 with 1 M NaOH) and centrifuged to remove entrained salt solution. Two more ethanol washes were conducted without pH adjustment. Two samples were removed, dispersed in 15 mL of MilliQ water, frozen immediately at −80°C, and then freeze dried for solid phase analysis. Four replicate samples were resuspended in 33.0 g of 0.1 *m* $Mg(NO_3)_2$, shaken for 1 h and then centrifuged at 28,700 *g* for 20 min to extract "exchangeable" Cs and Sr. The supernatant solution was collected and acidified with concentrated HNO_3 to pH 2 before analysis. Pellets were then washed three times with 95% ethanol before being resuspended in 0.2 *m* acidic ammonium oxalate solution (AAO) (4 h at pH 3 on a reciprocal shaker in the dark) to extract "poorly-crystalline" precipitates (Jackson et al., 1986). The samples were centrifuged at 28,700 *g* for 20 min and the supernatant solution was acidified to pH 1.

2.3. Solution Phase Analysis

An Accumet solid state electrode with a Si-free glass bulb was calibrated by Gran titration of a 1.0 *m* NaOH solution at 2 *m* ionic strength ($NaNO_3$ background) using standardized HCl to allow direct measurement of H^+ concentration in each of the reacted STWL solutions. Concentrations of Si, Al, Fe, Cs and Sr in supernatant and AAO solutions were determined by inductively coupled plasma (ICP) atomic emission spectrometry (AES, Thermo Jarrell Ash Model 61E) or ICP mass spectrometry (MS, Perkin Elmer Model DRC II). Clay-free control samples reacted for one year were analyzed for dissolved inorganic C (DIC) using a Shimadzu TOC/TN analyzer to assess diffusion of CO_2 into the reaction vessels; DIC values were consistently <2 mM.

3. RESULTS

3.1. Composition of the Purified Clays

Selected physical-chemical data on the purified clays are presented in Tables 1 and 2. For illite, both the chemical formula and the ratio of accessible to total structural charge ($\sigma_{0,expt}/\sigma_{0,calc}$) indicate that a large fraction of the charged sites remain balanced by K^+ occupancy in collapsed interlayers (Table 1) and most of this illite structural charge is inaccessible to adsorptive Cs (Table 2). The ratio $\sigma_{0,expt}/\sigma_{0,calc}$ increases from 0.03 for illite to 0.1 for vermiculite and 0.45 for montmorillonite (Table 2), which is consistent with the measured increase in total specific surface area, relative to illite, for vermiculite (2.1 times) and montmorillonite (7.5 times), and with the increased interlayer accessibility to aqueous phase ions (SSA_{EGME}, Table 1). Also noteworthy is the high Al for Si substitution in the vermiculite tetrahedral sheet, relative to illite and montmorillonite (Table 1). Total digests of the Na-saturated clays revealed no detectable native Cs, low native Sr in vermiculite (0.07 mmol kg^{-1}) and montmorillonite (0.09 mmol kg^{-1}), but higher native Sr (2.5 mmol kg^{-1}) in illite.

3.2. Clay Dissolution and Precipitation Dynamics

Solution $-\log[H^+]$ values were relatively consistent over the full set of experimental conditions and sampling periods, mostly falling between 13.5 and 13.7, in systems comprising illite (Il), vermiculite (Vm) and montmorillonite (Mt), as well as in clay-free controls. However, there was significant variation among the clays, co-contaminant concentrations and time, in respect to Al, Si and Fe dynamics (Figs. 1–3). In all cases, the concentration of soluble Si increased initially with time, reached a maximum at 190 d (Il) or 33 d (Vm and Mt), and subsequently decreased up to 93 d (Mt) or 369 d (Il and Vm) systems (Fig. 1). Re-solubilization of Si between 190 and 369 d was observed in Mt systems at low and intermediate Cs/Sr concentration (Fig. 1e), concurrent with near complete removal of dissolved Al in these systems (Fig. 2e). Overall, the Si dissolution rate increased in the order Il < Vm < Mt. For Il, time-dependent Si dissolution patterns were similar for low and intermediate Cs and Sr concentrations (10^{-5} and 10^{-4} *m* Cs/Sr) (Fig. 1a), but dissolution was suppressed at high (10^{-3} *m*) Cs/Sr. Similar suppressive effects of Cs/Sr on Si release were

Table 2. Calculated layer charge and Cs^+-accessible charge before and after Na^+ exchange (0.01 *m* NaCl at pH 7).

Clay Mineral	Layer Charge[3] ($-\sigma_{0,cal}$)	$q_{Cs\ max}$[4]	$q_{Cs,Na1}$[2] ($-\sigma_{0,expt}$)	$q_{Cs,\ Na2}$[2]
	[$mmol_c\ kg^{-1}$]			
Illite (IMt-1)	2750 ± 15	151 ± 2.87	90 ± 2.15	68.0 ± 0.73
Vermiculite	1970 ± 10	271 ± 6.80	191 ± 2.04	159 ± 1.48
Montmorillonite (SWy-2)	1380 ± 18	783 ± 0.63	627 ± 5.22	538 ± 7.23

[3] Calculated from chemical formula.
[4] Cesium adsorption capacity ($q_{Cs,max}$), Cs accessible structural charge ($\sigma_{0,expt}$), and $q_{Cs,Na2}$ were determined by measuring the surface excess of Cs after clay surface saturation by repeated washing with a CsCl solution ($q_{Cs,max}$), saturation followed by one Na exchange step ($q_{Cs,Na1} = -\sigma_{0,expt}$), and saturation followed by two Na exchange steps ($q_{Cs,Na2}$), according to Chorover et al. (1999)

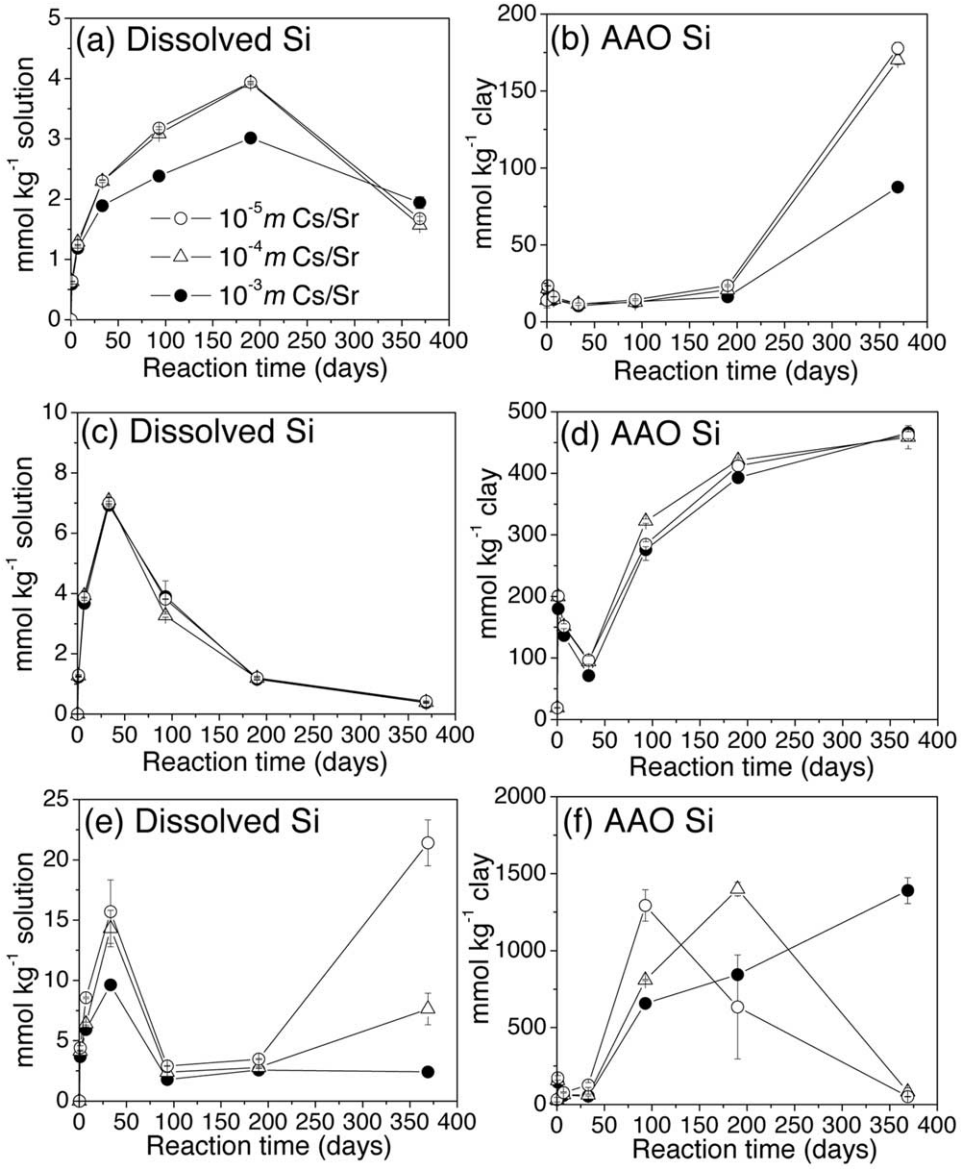

Fig. 1. Time-dependent changes in dissolved Si and acid ammonium oxalate extractable (AAO) Si in solid products from (a, b) illite, (c, d) vermiculite and (e, f) montmorillonite at initial solution concentrations of 10^{-5}, 10^{-4} and 10^{-3} mol kg^{-1} Cs/Sr. Error bars indicate standard deviations for duplicate samples.

observed for Mt (Fig. 1e), whereas little effect was observed for Vm (Fig. 1c).

Acidic ammonium oxalate (AAO) extraction targets poorly-crystalline, short-range-ordered or otherwise acid-soluble solids that precipitate in response to the elevated Si concentrations induced by clay mineral dissolution (Fig. 1). All clays show a small increase in AAO extractable Si during the first day of reaction, followed by a small initial decrease, and then a large increase over longer times (Fig. 1). Onset of the increase in AAO is coincident with maximum dissolved Si, and the rate of accumulation in AAO extractable solids corresponds to the preceding rate of Si release. For example, the rate of accumulation of AAO Si from Il is lower for 10^{-3} *m* Cs/Sr than for the 10^{-5} or 10^{-4} *m* Cs/Sr cases (Fig. 1b), as is the Si release rate (Fig. 1a). A maximum, followed by subsequent decline, in AAO extractable Si is reached for Mt systems (Fig. 1f) at low and intermediate co-contaminant concentration (10^{-5} and 10^{-4} *m* Cs/Sr) systems, which also show the highest Si dissolution rates (Fig. 1e). The maximum is reached at 90 d for 10^{-5} *m* Cs/Sr and 190 d for 10^{-4} *m* Cs/Sr. No maximum in AAO Si is observed for the 10^{-3} *m* Cs/Sr case, nor for the other clays, within the time frame of the experiment. In Mt, the time to maximum AAO Si increases with increasing Cs/Sr concentration (Fig. 1f). The reduction in AAO Si occurs in concert with an apparent solubilization of a comparable mass of Si (Fig. 1e). In the case of Vm (Fig. 1c), neither the rate of Si release (Fig. 1c) nor its accumulation in AAO extractable solids was affected by initial Cs and Sr loading.

Whereas initial (t = 0) solutions are devoid of Si and all evolving Si (Fig. 1) derives from clay mineral weathering, STWL concentrations of Al are relatively high (*ca.* 0.05 *m* at t = 0) from

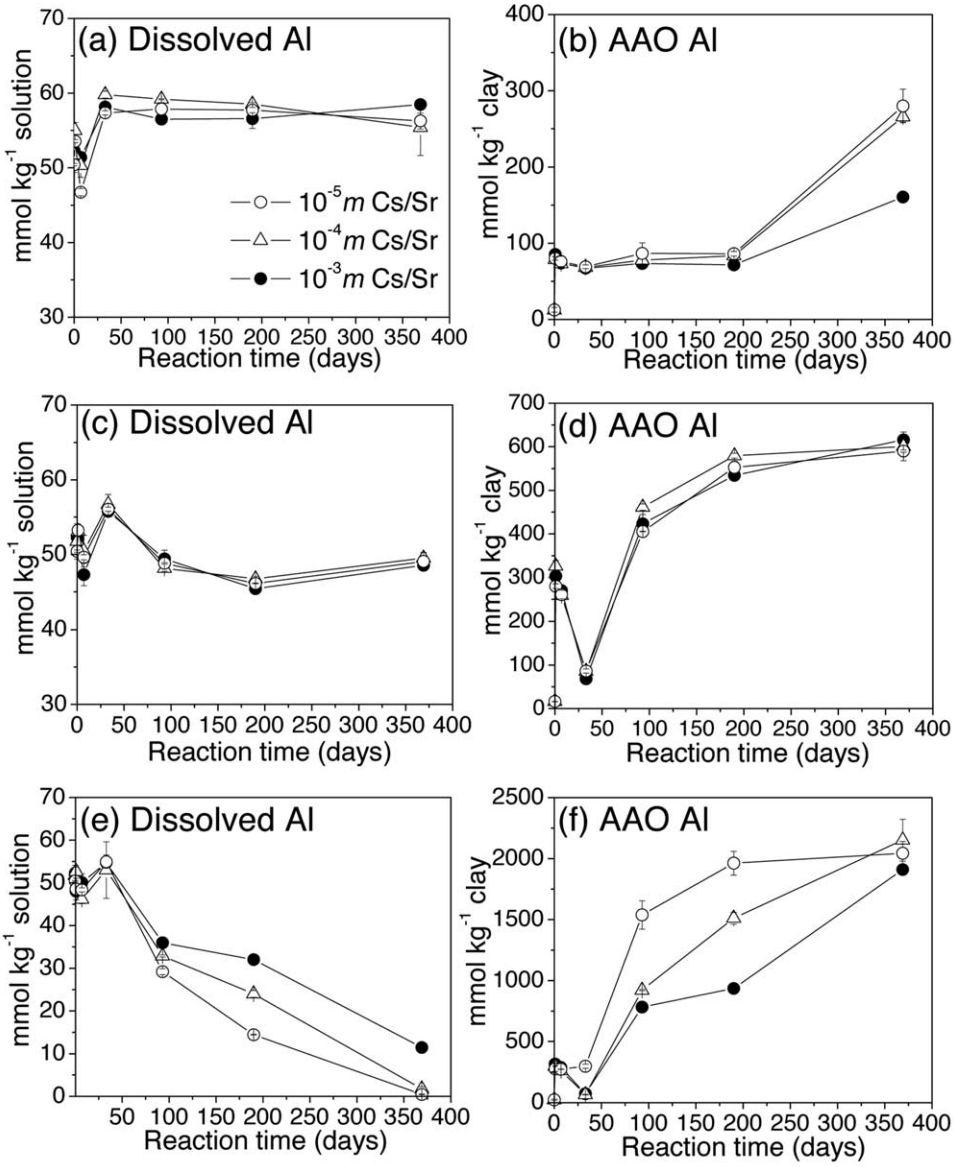

Fig. 2. Time-dependent changes in dissolved Al and AAO extractable Al in solid products from (a, b) illite, (c, d) vermiculite, and (e, f) montmorillonite at initial solution concentrations of 10^{-5}, 10^{-4} and 10^{-3} mol kg^{-1} Cs/Sr. Error bars indicate standard deviations for duplicate samples.

the outset (Fig. 2). Dissolved Al decreases at first and then increases to a maximum value at 33 d, followed by a decline, for which the rate and extent vary depending on the clay (Fig. 2). The decline is small for Il (Fig. 2a) and Vm (Fig. 2c), which show final concentrations at 369 d that are comparable to initial values. Nonetheless, there is a significant accumulation of Al in SRO solids for these two clays (Fig. 2b and 2d), with a time-dependency that matches that seen for Si (Fig. 1b and 1d).

Given the solid to solution mass ratio of 1:50, maximum values of AAO Al (Fig. 2) following 369 d reaction represent incorporation of Al into extractable solids at levels equivalent to 7%–12% (Il), 23%–25% (Vm) and 76%–86% (Mt) of that present initially in STWL. This increasing uptake of AAO Al (Il < Vm < Mt) correlates with the initial rate of Si dissolution, suggesting that Si release rate controls Al sequestration from solution, and, therefore, the overall rate of secondary aluminosilicate formation. Similar to the case for Si (Fig. 1), a suppressive effect of Cs/Sr concentration on accumulation of AAO Al is evident for Il (Fig. 2b) and especially Mt (Fig. 2f), whereas no effect is observed for Vm (Fig. 2d). This co-contaminant effect results from the influence of Cs/Sr on Si dissolution rate; the highest initial rate of Si dissolution (Mt, 10^{-5} *m* Cs/Sr, Fig. 1e) results in the fastest removal of Al from solution (Fig. 2e) and its accumulation in AAO Al (Fig. 2f). However, unlike AAO Si, which increases to a maximum followed by a subsequent decline in Mt at 10^{-5} and 10^{-4} *m* Cs/Sr (Fig. 1f), AAO Al continues to accumulate up to 369 d, converging for all three Cs/Sr concentrations upon approaching 90% removal of dissolved Al (Fig. 2f).

Dissolved and AAO extractable masses of clay-derived Fe (Fig. 3) are much lower than comparable values for Si and Al, as

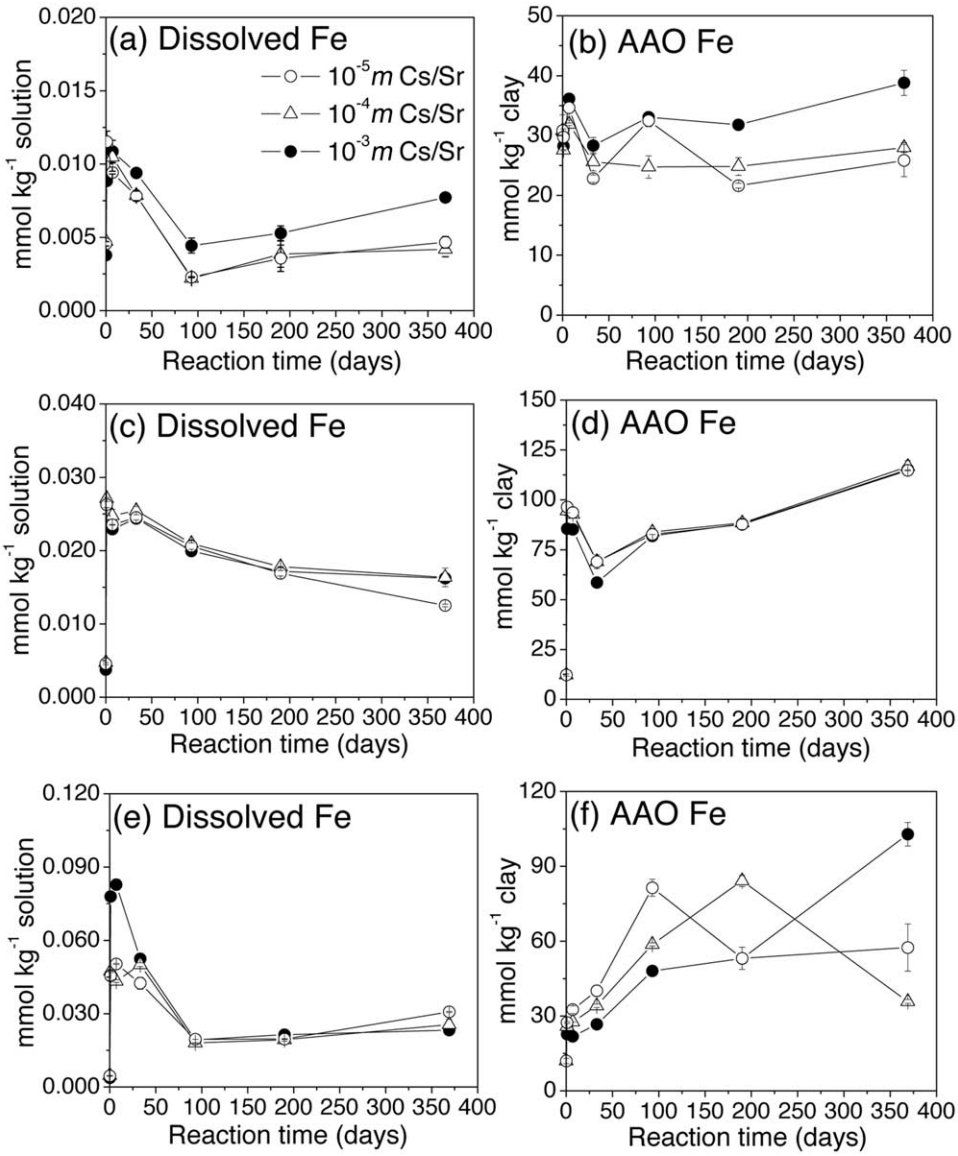

Fig. 3. Time-dependent changes in dissolved Fe and AAO extractable Fe in solid products from (a, b) illite, (c, d) vermiculite, and (e, f) montmorillonite at initial solution concentrations of 10^{-5}, 10^{-4} and 10^{-3} mol kg^{-1} Cs/Sr. Error bars indicate standard deviations for duplicate samples.

expected from the clay chemical formulae (Table 1). However, dissolution and re-precipitation reactions are quite rapid. Furthermore, the time-dependencies and effects of Cs/Sr concentration on Fe release and accumulation in AAO extractable forms are similar to those observed for Si (Fig. 1).

3.3. Contaminant Uptake and Release

No significant changes with time in aqueous phase concentrations of Cs, Sr or Al were observed in the clay-free controls, with or without Al addition, indicating that sorption to vessel walls was negligible (data not shown). Also, no precipitation reactions were detected in the absence of clay. The kinetics of clay mineral dissolution were coupled to long-term Cs and Sr uptake (Fig. 4), referred to herein as *sorption*, which may include adsorption and/or precipitation. Complete removal from solution would give sorbed amounts of 0.5, 5.0 and 50.0 mmol kg^{-1} for initial solution phase concentrations of 10^{-5}, 10^{-4} and 10^{-3} *m*, respectively.

Significant mass fractions of both Cs and Sr were sorbed in all cases, despite the high (2 *m*) background ionic strength (Fig. 4). Cs sorption at the two lower contaminant concentrations (10^{-5} and 10^{-4} *m*) increased in the order of Mt < Vm < Il. Sorption to Il was nearly complete at the lowest initial concentration (10^{-5} *m*) and fractional uptake decreased with increasing initial concentration. Distribution coefficients (K_d) for Cs on Il were 148 and 46 ($kg_{solution}$ $kg^{-1}{}_{solid}$) after 369 d of reaction time at initial Cs concentrations of 10^{-4} and 10^{-3} *m*, respectively. At the highest Cs loading in our experiments, sorption to Il appeared to be limited by site availability. Al-

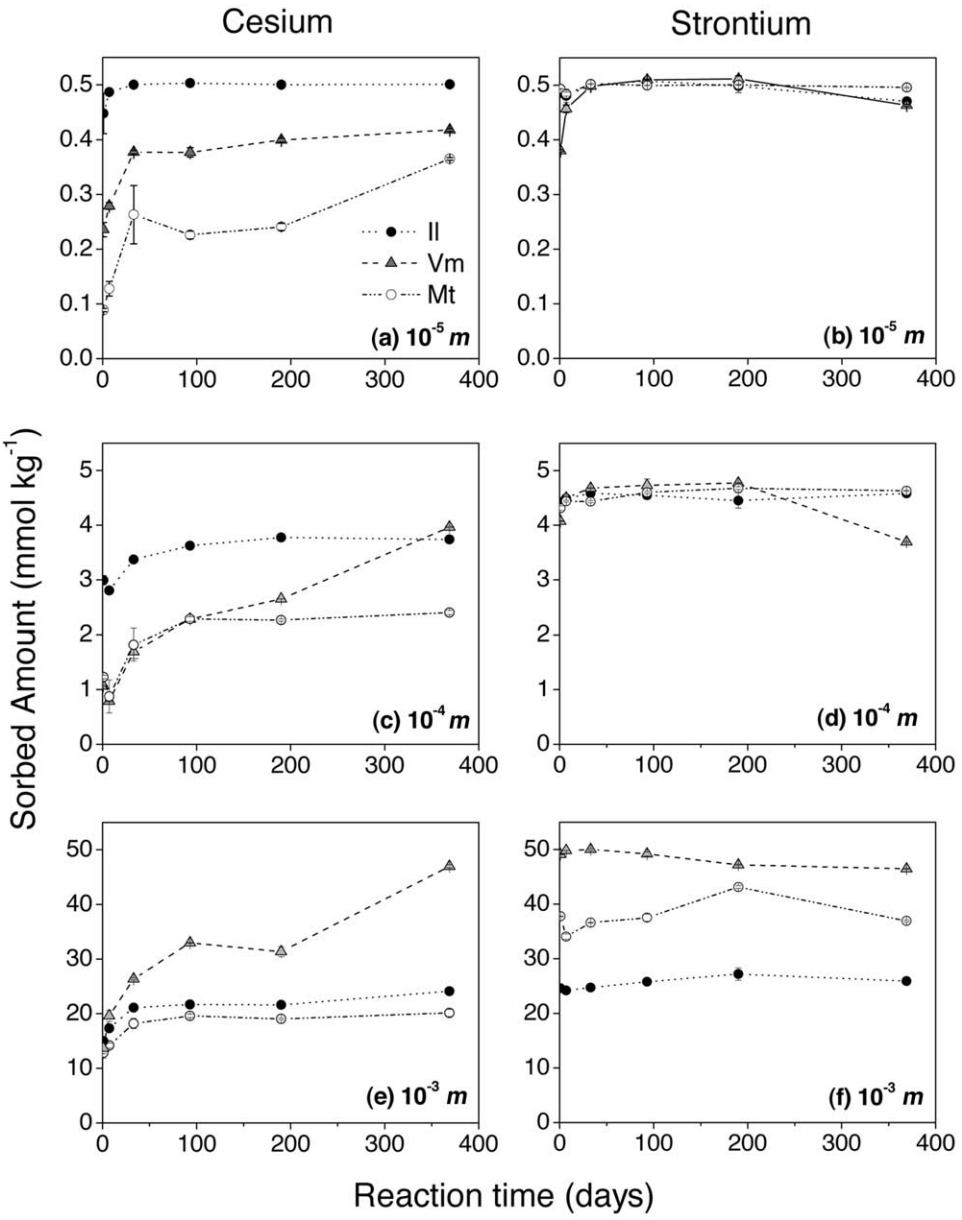

Fig. 4. Uptake dynamics of Cs and Sr in specimen clay systems, measured on the basis of loss from solution relative to mineral-free blanks. All clays are shown on each graph for comparison. Total initial aqueous concentrations are indicated in the bottom right of each graph. Complete removal from solution would give sorbed amounts of 0.5, 5.0 and 50.0 mmol kg^{-1} for initial solution phase concentrations of 10^{-5}, 10^{-4} and 10^{-3} *m*, respectively.

though fractional uptake of Cs was reduced for the higher initial concentrations, there was a clear long-term kinetic effect that contributed to a slow uptake reaction, particularly in the case of Vm (Fig. 4). In Mt, continuous Cs uptake was observed over reaction time and more rapid sorption occurred at the lowest Cs loading. In contrast, uptake of Sr was more rapid and complete for all clay systems at 10^{-5} and 10^{-4} *m* initial concentrations (Fig. 4b, d), whereas at the highest concentration, fractional uptake was diminished, except for Vm. At 10^{-3} *m* Cs/Sr, retention of Sr was greatest for Vm, followed by Mt and Il (Fig. 4f). Almost complete removal from solution was observed at 10^{-4} *m* in Il (Fig. 4d), but fractional uptake was reduced to near 60% at the highest initial loading (Fig. 4f). Vermiculite appears to be an especially effective sorbent for Sr as uptake was nearly complete even at the highest Cs and Sr loading (Fig. 5d–f). After 369 d, Sr sorption amounted to 99%, 93 and 74% removal from solution in Mt systems for initial concentrations of 10^{-5}, 10^{-4} and 10^{-3} *m*, respectively (Fig. 4).

Recovery of these contaminants from the solid phase are shown in the bar graphs (Fig. 5–7). The full height of bars in these figures indicates the total number of moles of Cs or Sr retained per unit initial mass of clay. The dotted line indicates the mass recovery expected after complete removal from solution (sorbed fraction = 1.0) of the added Cs or Sr. The mass

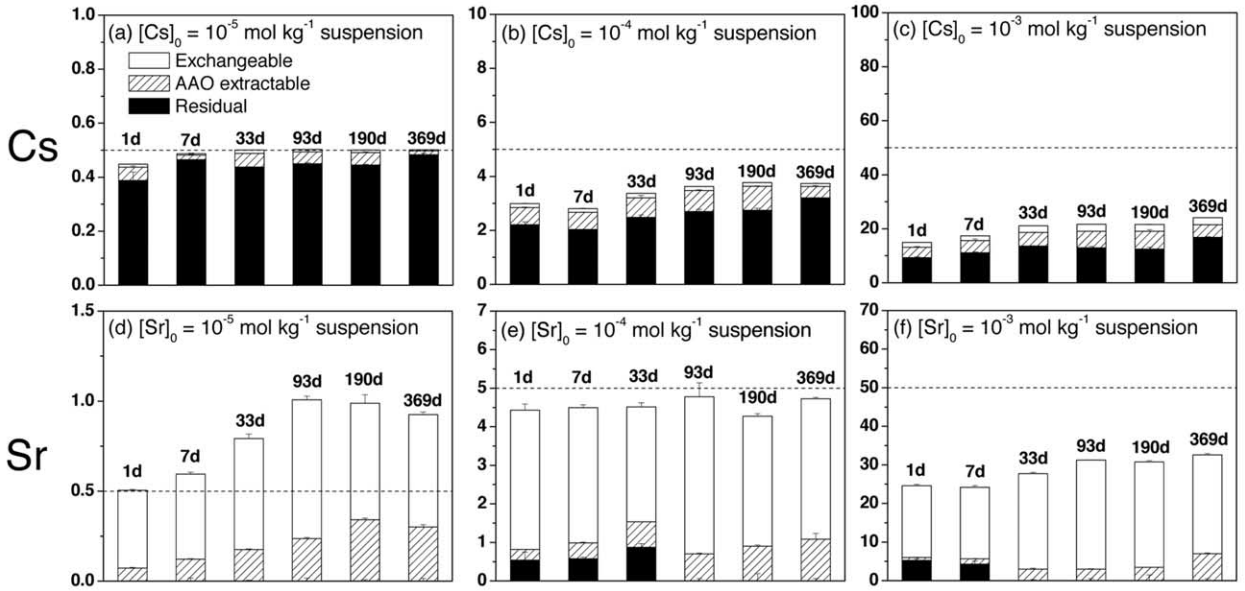

Fig. 5. Partitioning of sorbed Cs and Sr during incongruent dissolution of illite in STWL. Total bar height represents millimoles of Cs and Sr sorbed to the solid phase per kilogram of illite present initially (determined from concentration depletion in the aqueous phase). Complete removal from solution is represented by the horizontal lines at 0.5, 5.0, and 50.0 mmol kg^{-1} for initial aqueous contaminant concentrations of 10^{-5}, 10^{-4}, and 10^{-3} mol kg^{-1}, respectively. The millimoles of Cs and Sr recovered during Mg^{2+} exchange and AAO extraction are indicated, as is the unrecovered or "residual" mass. Error bars show standard deviations of replicate measurements. Excess recovery of Sr in (d) after 1 d results from increasing solubility of native Sr in IMt-1 (total concentration in clay = 2.6 mmol kg^{-1}).

fractions of each ion that are (i) desorbed by Mg exchange, (ii) dissolved by AAO extraction or (iii) non-extractable (residual) are differentiated by the stacked bars. The scales increase from left to right in each figure because of the increase in initial Sr and Cs concentrations. In all clays, a substantial mass fraction of Cs was resistant to removal by both Mg exchange and AAO extraction, resulting in a large "residual" pool. Furthermore, the amount of Cs sorbed into the residual fraction tends to increase over the course of the experiment. In Il, the relative proportion of "residual" Cs decreased with increasing initial Cs concentration, consistent with a limited number of high affinity sites, whereas in Vm and Mt, overall distribution of Cs into ex-

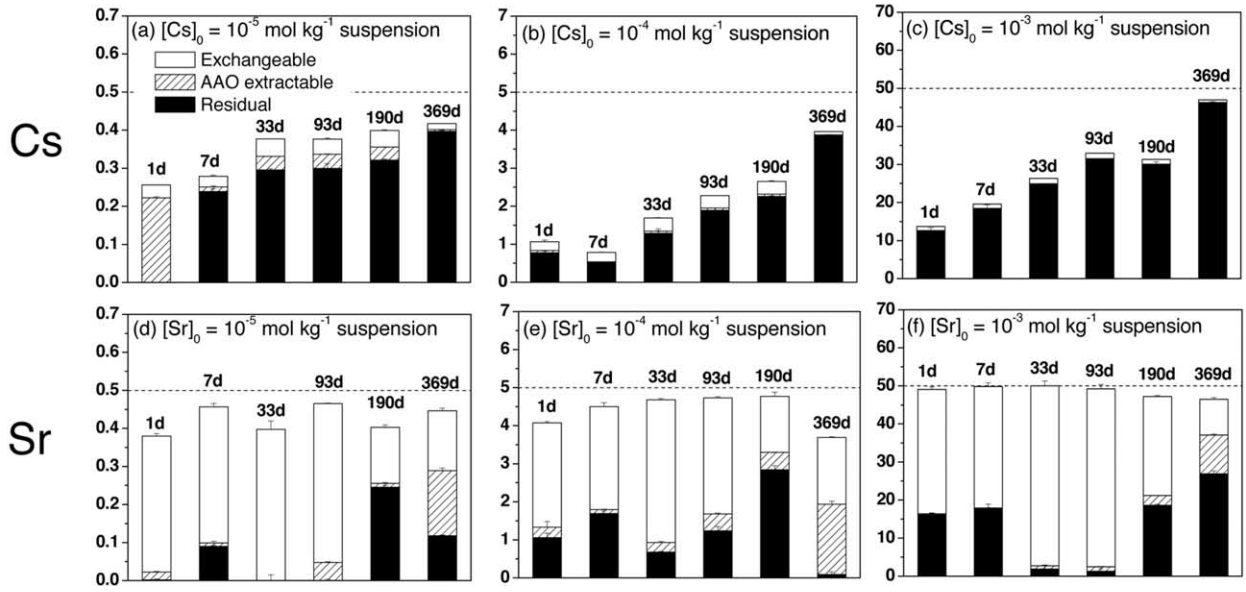

Fig. 6. Partitioning of sorbed Cs and Sr (mmol kg^{-1} clay) during incongruent dissolution of vermiculite in STWL (other information as in Fig. 5).

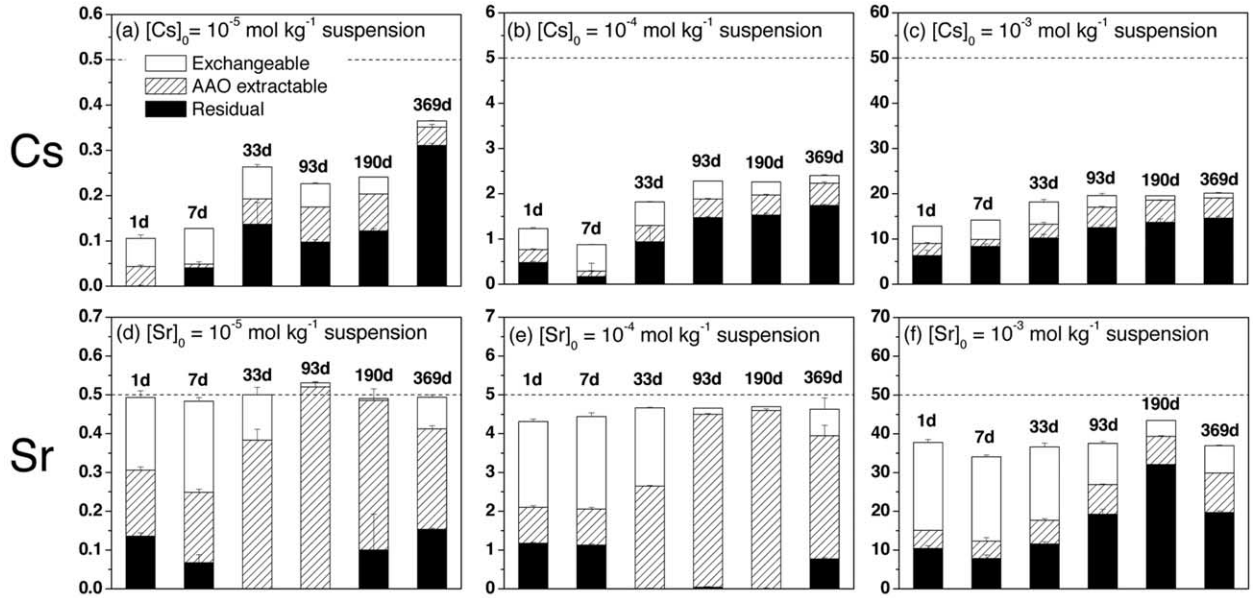

Fig. 7. Partitioning of sorbed Cs and Sr (mmol kg^{-1} clay) during incongruent dissolution of montmorillonite in STWL (other information as in Fig. 5).

changeable, AAO extractable and residual pools was relatively consistent over a wide (100-fold) variation in initial Cs concentration. However, there was an increase in AAO and residual pool concentrations with increasing reaction time, particularly in Mt (Fig. 7c). After 1 d in Vm systems, Cs was present dominantly in either Mg-exchangeable (small fraction) or non-extractable (large fraction) pools, whereas both Il and Mt systems consistently released a portion of Cs during AAO extraction.

At the lowest initial concentration (10^{-5} *m*), Sr recovery by Mg exchange and AAO extraction exceeded the added amount, indicating that some portion of the native 2.6 mmol kg^{-1} Sr in the Il sample had been mobilized by reaction with STWL (Fig. 5d). In the Il systems, most sorbed Sr was removed by unbuffered $Mg(NO)_3$ solution irrespective of initial concentration or reaction stage. In stark contrast to results for Cs, no residual Sr was evident after 93 d (Fig. 5d–f). However, AAO-extractable Sr increased in all Il systems with aging time. For Vm, Sr was mostly Mg-exchangeable at early times (before 93 d for 10^{-5} and 10^{-4} *m* and before 190 d for 10^{-3} *m* initial Cs and Sr concentrations), but later was incorporated into AAO extractable and residual pools (Fig. 6d–f). This "aging" effect was even more pronounced in the case of Mt, where Mg-exchangeable Sr was converted to increasingly recalcitrant AAO extractable and residual forms over the one-year reaction period (Fig. 7d–f), comparable to prior studies of kaolinite (Chorover et al., 2003). The mass of Sr incorporated into AAO extractable or residual form increases in the order Il < Vm < Mt, consistent with the extent of weathering-induced transformation of these solids as measured by aqueous Si and Al dissolution and reprecipitation (Fig. 1–2). In Mt, the formation of residual Sr was favored by higher initial Sr concentrations, which suggests co-precipitation of Sr in neoformed solids (Fig. 7f).

4. DISCUSSION

The 2:1 layer-type clay minerals studied here are micaceous weathering products representing a range of interlayer expansion, specific surface area (SSA), and tetrahedral vs. octahedral charge properties. In this work, we observed an increase in clay Si release with increasing SSA from illite to montmorillonite. However, SSA is not the sole predictor of dissolution rate, since a comparable study (Chorover et al., 2003) with lower SSA kaolinite (KGa-2, SSA = 39 m^2 g^{-1}) gave higher initial Si release and AAO Si accumulation rates than observed for any of the 2:1 clays.

4.1. Dissolution-Precipitation Reactions

At high pH and in a concentrated $NaNO_3$ background, parallel adsorption and precipitation reactions compete for the fate of aqueous phase Cs and Sr. Unlike experiments where ion adsorption is measured on time scales that are short relative to the kinetics of mineral weathering processes, the caustic, high Al background solutions employed in this work induce dissolution of Si (Fig. 1) and Fe (Fig. 3) and their co-precipitation with Al (Fig. 2) such that mineral transformations may drive contaminant-solid phase associations (Fig. 5–7). Incorporation of contaminant ions into neoformed reaction products depends not only on the rate of Si release from clay dissolution and its re-precipitation in solid phase products, but also on Cs or Sr affinity for the parent clay, reaction time, and initial contaminant concentration (Fig. 5–7).

The availability of Al exerts significant control over the mass of dissolved Si, and therefore, the uptake by neoformed Al/Si solids of Cs and Sr as well. This is illustrated by the fact that the increase in dissolved Si after 200 d in Mt (10^{-5} and 10^{-4} *m* in Fig. 1e) is coincident with the complete removal of Al from aqueous solution. This indicates that the cause of the

resurgence in aqueous phase Si in the Mt systems is exhaustion of the secondary aluminosilicate "sink". In other words, Si accumulates in solution at this late stage of reaction because its precipitation into solid phase products is limited by the diminished availability of co-precipitating Al. This renewed dissolution of Si thus appears to derive from montmorillonite, rather than re-solubilization of the neoformed aluminosilicate species. This finding is also supported by detailed mineralogical analyses reported in the companion paper (Choi et al., 2005). The secondary solids are observed to become increasingly resistant to oxalate-promoted dissolution with increased aging time (Fig. 1f, 2f, 3f; Chorover et al., 2003; Choi et al., 2005).

4.2. Contaminant Sequestration

Prior studies have shown that Cs exhibits a high affinity for frayed edge sites (FES) in illite (Sawhney, 1972) and in illitic Hanford sediments even at ionic strengths approaching 7 mol L^{-1} (Zachara et al., 2002) and this is attributed to inner-sphere complex formation of Cs^+ at high affinity siloxane sites (Kim et al., 1996; Kim and Kirkpatrick, 1997). Comans and coworkers observed that Cs sorption to illite was characterized by initially rapid uptake followed by slower "secondary" sorption on time scales of weeks to months or longer, and that sorption reversibility was diminished with reaction time (Comans et al., 1991; Comans and Hockley, 1992). They attributed the slow kinetic to diffusion-limited migration of Cs to interlayer sites. McKinley et al. (2004) observed preferential adsorption of Cs to FES and found that Cs also penetrated the interior of mica particles into zones of K depletion, presumably by migration along channels within the crystals. In the present work, the decreased fractional uptake at high Cs concentration and slow secondary sorption of Cs (Fig. 4), is consistent with limited FES availability in Il.

Slow Cs sorption to Vm was also observed (Fig. 4) and this was coupled to extensive uptake, the highest of all the clays studied at 369 d. This behavior derives from the high tetrahedral-sheet charge density and limited interlayer expansibility of this mineral, which is intermediate between illite and montmorillonite. In a seminal study, Sawhney (1966) reported rapid Cs uptake to Ca saturated montmorillonite, whereas uptake to vermiculite was characterized by a fast initial step, followed by slow and extensive uptake over a 21 d period at circumneutral pH. Analogous results have been reported in a comparative study of K sorption to montmorillonite and vermiculite, with the latter exhibiting slower and more extensive secondary uptake (Jardine and Sparks, 1984). Like these investigators, we attribute the rapid initial sorption of Cs on Vm to external basal surfaces and edge sites, whereas the slow uptake is attributed to Cs diffusion into the interlayers. Slow gradual uptake during the reaction time in Vm is possibly induced by a particle size effect.

Sorbed Cs was largely non-extractable by Mg exchange and AAO treatment, especially for Il (Fig. 5) and Vm (Fig. 6) throughout the reaction time. Given that Si and Al precipitates were more readily dissolved (Fig. 1–2), these results suggest that strong Cs binding to illite FES and the vermiculite interlayer (Sikalidis et al., 1988) persists even after 1 y reaction time in the caustic conditions representative of tank waste solutions at the Hanford site. Although it is plausible that Cs adsorption to the vermiculite siloxane surface induced partial interlayer collapse, resulting in subsequent diffusion limited uptake, basal (*d*-001) spacings measured by X-ray diffraction (Choi et al., 2005) were slightly increased over the reaction time, consistent with concurrent uptake of both Cs and hydrated Sr. In molecular simulations, Sutton and Sposito (2001) observed tightly bound Cs^+ at tetrahedral-charge sites, and suggested that these sites have a dominating influence on interlayer species in a mixed-charge-distribution clay mineral. In our experiments, tetrahedral charge is most prevalent in vermiculite (Table 1), which explains its greatest capacity for strong retention of Cs even at the highest concentrations (Fig. 6c).

Although Sr sorption exceeded that of Cs in all cases (Fig. 4), it was also more readily desorbed in the subsequent extractions (Figs. 5–7). The observation, that Sr exhibited its greatest recalcitrance to desorption/dissolution in Mt (Fig. 7), is apparently coupled to the more extensive Si dissolution (Fig. 1) and re-precipitation with Al (Fig. 2) that occurred in that system. Single particle analyses by TEM-EDS (Choi et al., 2005) indicate Sr incorporation into these precipitates. The more rapid Si release rate in Mt effectively removed nearly all of the Al from solution during precipitate formation (Fig. 2e-f). In contrast, solution phase Al concentrations remained relatively constant in Il and Vm despite the accumulation of AAO Al, suggesting that the solution phase behaves as a conduit by transferring Al from clay to secondary precipitates.

In Mt, higher concentrations of Cs and Sr were found to diminish the rate of clay Si release, slow its co-precipitation with Al, and decrease the rate at which these precipitates converted to non-extractable (i.e., "more crystalline") solids. This result is similar to what was observed for kaolinite, which also exhibited a high dissolution rate (Chorover et al., 2003). For kaolinite, the time required to reach maximum AAO Si increased from 33 to 190 d as Cs and Sr concentrations increased from 10^{-5} to 10^{-3} *m*, whereas the comparable times to AAO Si maxima for Mt increase from 90 to 369 d with increasing Cs and Sr (Fig. 1f). In both cases, the subsequent decrease in extractable Si is attributable to the formation of dissolution-resistant, crystalline secondary solids (Chorover et al., 2003; Choi et al., 2005). These results suggest that higher concentrations of Cs and Sr in solution inhibit crystallization process. Research into the mechanism(s) of Cs/Sr control over mineral transformation rates, as observed here for Mt and Il and previously for kaolinite (Chorover et al., 2003), is a priority for current work in our lab.

Despite the longer-term persistence of AAO labile Si, Al and Fe bearing solids in Mt at the higher Sr concentration (Fig. 1f, 2f, 3f), Sr itself showed diminished solubility in AAO in the same systems (Fig. 7), and a large fraction was not recovered from the solid phase. This suggests that Sr-bearing precipitates may be discrete from the dominant Al-Si phase "signal", or that the rapid initial sorption of Sr to clay particles results in its occlusion under poorly-crystalline coatings that are incompletely removed by AAO. Microscopic and spectroscopic studies of the product solids in a companion paper (Choi et al., 2005) provide evidence for both of these mechanisms.

5. CONCLUSIONS

Interlayer accessibility, charge location and weathering dynamics affect long-term uptake and retention of Cs and Sr in suspensions subjected to caustic HLRW leachate. Dissolution rates of 2:1 layer-type clays reacted with a synthetic tank waste leachate solution (STWL, pH 14, 2 M $NaNO_3$, 50 mM Al) are greatest for montmorillonite (Mt), followed by vermiculite (Vm) and illite (Il). Rates of mineral transformation and the formation of dissolution-resistant secondary phases, as measured by solubility dynamics of Al and Si, are diminished by increasing initial Cs and Sr concentrations in Mt systems, whereas a smaller effect of co-contaminant concentration is observed for illite and vermiculite. Despite the extreme geochemical conditions imposed in the present work, Cs uptake behavior at high pH and ionic strength exhibits trends that are similar macroscopically to prior studies at circumneutral pH; rapid initial sorption is followed by a slower consistent accumulation of sorbate. However, the mechanism of slow uptake appears to be specific to the type of clay mineral. The data suggest interlayer diffusion limits uptake rates in Il and Vm, while co-precipitation in secondary solids may be more important in reacted Mt. Strontium uptake is more rapid, and resistance to subsequent desorption correlates with the rate and extent of mineral transformation, which follows the order Mt > Vm > Il. The results indicate that both sorption to clay mineral surfaces and incorporation into neoformed secondary solids control the fate of Cs and Sr in soils and sediments subjected to the extreme geochemical conditions of HLRW.

Acknowledgments—We are grateful to B. Baeyens, an anonymous reviewer, and Associate Editor D. L. Sparks for constructive comments on an earlier draft. This research was supported by the Environmental Management Science Program of the Office of Science, U. S. Department of Energy, grants DE-FG07-99ER15012 and DE-FG07-02ER63504.

Associate editor: D. L. Sparks

REFERENCES

Bailey S. W. (1980) Structures of the layer silicates. In *Crystal Structures of the Clay Minerals and Their X-ray Identification* (eds. G. W. Brindley and G. Brown), pp. 1–124. Monogr. No. 5, Mineralogical Society, London.

Bickmore B. R., Nagy K. L., Young J. S. and Drexler J. W. (2001) Nitrate-cancrinite precipitation on quartz sand in simulated Hanford tank solutions. *Environ. Sci. Technol.* **35,** 4481–4486.

Bostick B. C., Vairavamurthy M. A., Karthikeyan K. G. and Chorover J. (2001) Cesium adsorption on clay minerals: An EXAFS spectroscopic investigation. *Environ. Sci. Technol.* **36,** 2670–2676.

Chen C. -C., Papelis C. and Hayes K. F. (1998) Extended X-ray absorption fine structure (EXAFS) analysis of aqueous Sr(II) ion sorption at clay-water interfaces. In *Adsorption of Metals by Geomedia* (ed. E. A.) Vol. Jenne 333, pp. 333–348. Academic Press, NY.

Choi S., Crosson G., Mueller K. T., Seraphin S. and Chorover J. (2005) Clay mineral weathering and contaminant dynamics in a caustic aqueous system. II. Mineral transformation and microscale partitioning. *Geochim. Cosmochim. Acta* **69** (*18*), 4473–4487.

Chorover J., Dichiaro M. J. and Chadwick O. A. (1999) Structural charge and cesium retention in a chronosequence of tephritic soils. *Soil Sci. Soc. Am. J.* **63,** 169–177.

Chorover J., Choi S., Amistadi M. K., Karthikeyan K. G., Grosson G. and Mueller K. T. (2003) Linking cesium and strontium uptake to kaolinite weathering in silmulated tank waste leachate. *Environ. Sci. Technol.* **37,** 2200–2208.

Chorover J., Rotenberg P. A. and Serne R. J. (2004) Mineral formation and radionuclide sorption in waste impacted Hanford sediments. In *Water-Rock Interaction* 11 (ed. R. Wanty and R. R. Seal II), pp. 675–678. A. A. Balkema Publishers, Leiden.

Cîćêl B., and Komadel P. (1994) Structural formulae of layer silicates. In *Quantitative Methods in Soil Mineralogy* (eds. J. E. Amonette and L. W. Zelazny) pp. 114–136. Madison, WI.

Comans R. N. J., Haller M. and Preter P. D. (1991) Sorption of cesium on illite: Non-equilibrium behavior and reversibility. *Geochim. Cosmochim. Acta* **55,** 433–440.

Comans R. N. J. and Hockley D. E. (1992) Kinetics of cesium sorption on illite. *Geochim. Cosmochim. Acta* **56,** 1157–1164.

Douglas L. A. (1989) Vermiculites. In *Minerals in Soil Environments, 2nd edition.* (eds. J. B. Dixon and S. B. Weed), pp. 635–674. SSSA Book Series No. 1. Madison, Wisconsin. Soil Science Society of America.

Dyer A., Chow J. K. K. and Umar I. M. (2000) The uptake of caesium and strontium radioisotope onto clays. *J. Mater. Chem.* **10,** 2734–2740.

Gutierrez M. and Fuentes H. R. (1993) Modeling adsorption in multicomponent systems using a Freundlich-type isotherm. *J. Contam. Hydrol.* **14,** 247–260.

Jardine P. M. and Sparks D. L. (1984) Potassium-calcium exchange in a multi-reactive soil system. I *Kinetics. Soil Sci. Soc. Am. J.* **48,** 39–45.

Jeong C. H., Kim C. S., Kim S. J. and Park S. W. (1996) Affinity of radioactive cesium and strontium for illite and smectite clay in the presence of groundwater ions. *J. Envir. Sci. Health A.* **31,** 2173–2192.

Kim Y., Cygan R. T. and Kirkpatrick R. J. (1996) Cs-133 NMR and XPS investigation of cesium adsorbed on clay minerals and related phases. *Geochim. Cosmochim. Acta* **60,** 1041–1052.

Kim Y. and Kirkpatrick R. J. (1997) ^{23}Na and ^{133}Cs NMR study of cation adsorption on mineral surfaces: Local environments, dynamics and effects of mixed cations. *Geochim. Cosmochim. Acta* **61,** 5199–5208.

Liu C., Zachara J. M., Smith S. C., Mckinley J. P. and Ainsworth C. C. (2003a) Desorption kinetics of radiocesium from subsurface sediments at Hanford Site, USA. *Geochim. Cosmochim. Acta* **67,** 2893–2912.

Liu C., Zachara J. M., Qafoku O. and Smith S. C. (2003b) Effect of temperature on Cs+ sorption and desorption in subsurface sediments at the Hanford site, USA. *Environ. Sci. Technol.* **37,** 2640–2645.

Lu N. and Mason C. F. V. (2001) Sorption-desorption behavior of strontium-85 onto montmorillonite and silica colloids. *Appl. Geochem.* **16,** 1653–1662.

Maes A. and Cremers A. (1978) Charge density effects in ion exchange. Part 2: Homovalent exchange equilibria *J. Chem. Soc. Faraday Trans. 1* **74,** 1234–1241.

McKinley J. P., Zachara J. M., Gassman P. L., Ainsworth C. C., Arey B., McKinley S., Shaef T., Smith S. C., Kimberling J., Bish D. L., Chipera S. J. and Snow P. (2002) S-SX site mineralogy. Section D. 2.0 in Field Investigation Report for Waste Management Area S-SX. RPP-7884, Rev. 0. Technical Report prepared for U.S. Department of Energy, Office of River Protection, Richland, WA.

McKinley J. P., Zeissler C. J., Zachara J. M., Serne R. J., Lindstrom R. M., Schaef H. T. and Orr R. D. (2001) Distribution and retention of ^{137}Cs at the Hanford Site, Washington. *Environ. Sci. Technol.* **35,** 3433–3441.

O'Day P. A., Newville M., Neuhoff P. S., Sahai N. and Carroll S. A. (2000) X-ray absorption spectroscopy of strontium(II) coordination. I. Static and thermal disorder in crystalline, hydrated and precipitated solids and in aqueous solution. *J. Coll. Interface Sci.* **222,** 184–197.

Oscarson D. W., Watson R. L. and Miller H. G. (1987) The interaction of trace levels of cesium with montmorillonitic and illitic clays. *Appl. Clay Sci.* **2,** 29–39.

Oscarson D. W., and Hume H. B. (1998) Effect of solid:liquid ratio on the sorption of Sr2+ and Cs+ on bentonite. In *Adsorption of Metals by Geomedia. Variables, Mechanisms, and Model Applications* (ed. E. A. Jenne). pp. 277–289. Academic Press, San Diego, CA.

Pennell K. D. (2002) Specific surface area. In *Methods of Soil Analysis, Part 4: Physical Methods* (eds. J. H. Dane and G. C. Topp) pp. 295–315. SSSA Book Series, Soil Science Society of America. Madison, WI.

Poinssot C., Baeyens B. and Bradbury M. H. (1999) Experimental and modeling studies of caesium sorption on illite. *Geochim. Cosmochim. Acta* **63,** 3217–3227.

Puls R. W., Ames L. L. and McGarrah J. E. (1989) The use of batch tests as screening tool for radionuclide sorption characterization studies, Hanford, Washington, U.S.A. *Appl. Geochem.* **4,** 63–77.

Rafferty P., Shiao S.-Y., Binz C. M. and Meyer R. E. (1981) Adsorption of Sr(II) on clay minerals: effects of salt concentration, loading and pH. *J. Inorg. Nucl. Chem.* **43,** 797–805.

Sahai N., Carroll S. A., Roberts S. and O'Day P. A. (2000) X-ray absorption spectroscopy of Sr(II) coordination. II. Sorption and precipitation at kaolinite, amorphous silica and goethite surfaces *J. Coll. Interface. Sci.* **222,** 198–212.

Sawhney B. L. (1966) Kinetics of cesium sorption by clay minerals. *Soil Sci. Soc. Am. Proc.* **30,** 565–569.

Sawhney B. L. (1972) Selective adsorption and fixation of cations by clay minerals: A review. *Clays Clay Miner.* **20,** 93–100.

Sawhney B. L. and Stilwell D. E. (1994) Dissolution and elemental analysis of minerals, soils and environmental samples. In *Quantitative Methods in Soil Mineralogy* (eds. J. E. Amonette and L. W. Zelazny) pp. 49–82. Soil Science Society of America. Madison, WI.

Serne R. J., Zachara J. M., and Burke D. S. (1998) Chemical information on tank supernatants, Cs adsorption from tank liquids onto Hanford sediments, and field observations of Cs migration from past tank leaks. PNNL-11495 US-510. Pacific Northwest National Laboratory, Richland, WA.

Serne R. J., Last G. V., Gee G. W., Schaef H. T., Lanigan D. C., Lindenmeir C. W., Clayton R. E., LeGore V. L., Orr R. D., Brown C. F., Burke D. B., Kutnyakov I. V., Wilson T. C. and Myers D. A (2001a) Geologic and Geochemical Data Collected from Vadose Zone Sediments from Borehole SX 41-09-39 in the S/SX Waste Management Area and Preliminary Interpretations. 162 p. Pacific Northwest National Laboratory, Richland, Washington.

Serne R. J., Schaef H. T., Bjornstad B. N., Williams B. A., Lanigan D. C., Horton D. G., Clayton R. E., LeGore V. L., O'Hara M. J., Brown C. F., Parker K. F., Kutnyakov I. V., Serne, J. N., Mitroshkov A. V., Last G. V., Smith S. C., Lindenmeier C. W., Zachara J. M. and Burke D. B (2001b) Characterization of Uncontaminated Sediments from the Hanford Reservation—RCRA Borehole Core Samples and Composite Samples. PNNL-2001-1. Pacific Northwest National Laboratory. Richland, Washington.

Sikalidis C. A., Misaelides P. and Alexiades C. A. (1988) Caesium selectivity and fixation by vermiculite in the presence of various competing cations. *Environ. Pollut.* **52,** 67–79.

Sposito G. and LeVesque C. S. (1974) Sodium-calcium-magnesium exchange on Siver Hill illite. *Clays Clay Miner.* **49,** 1153–1159.

Steefel C. I., Carroll S., Zhao P. and Roberts S. (2003) Cesium migration in Hanford sediment: a multisite cation exchange model based on laboratory transport experiments. *J. Contam. Hydrol.* **67,** 219–246.

Sutton R. and Sposito G. (2001) Molecular simulation of interlayer structure and dynamics in 12.4 Å Cs-smectite hydrates. *J. Coll. Interface Sci.* **237,** 174–184.

Torstenfelt B., Andersson K. and Allard B. (1982) Sorption of strontium and cesium on rocks and minerals. *Chem. Geol.* **36,** 123–137.

Zachara J. M., Smith S. C., Liu C., McKinley J. P., Serne R. J. and Gassman P. L. (2002) Sorption of Cs^+ to micaceous subsurface sediments from the Hanford site, USA. *Geochim. Cosmochim. Acta* **66,** 193–211.